



Article

A Physiological Approach to Explore How Thioredoxin–Glutathione Reductase (TGR) and Peroxiredoxin (Prx) Eliminate H₂O₂ in Cysticerci of *Taenia*

Alberto Guevara-Flores ¹, Gabriela Nava-Balderas ^{2,*}, José de Jesús Martínez-González ¹, César Vásquez-Lima ¹, Juan Luis Rendón ¹ and Irene Patricia del Arenal Mena ^{1,*}

¹ Departamento de Bioquímica, Facultad de Medicina, Universidad Nacional Autónoma de México (UNAM), Apartado Postal 70-159, Mexico City 04510, Mexico; guevarafa@bq.unam.mx (A.G.-F.); jjmtz@bq.unam.mx (J.d.J.M.-G.); cesarlima@ciencias.unam.mx (C.V.-L.); jrendon@bq.unam.mx (J.L.R.)

² Departamento de Microbiología y Parasitología, Facultad de Medicina, Universidad Nacional Autónoma de México (UNAM), Apartado Postal 70-159, Mexico City 04510, Mexico

* Correspondence: gabrielanavab@comunidad.unam.mx (G.N.-B.); darenal@bq.unam.mx (I.P.d.A.M.)

Abstract: Peroxiredoxins (Prxs) and glutathione peroxidases (GPxs) are the main enzymes of the thiol-dependent antioxidant systems responsible for reducing the H₂O₂ produced via aerobic metabolism or parasitic organisms by the host organism. These antioxidant systems maintain a proper redox state in cells. The cysticerci of *Taenia crassiceps* tolerate millimolar concentrations of this oxidant. To understand the role played by Prxs in this cestode, two genes for Prxs, identified in the genome of *Taenia solium* (*TsPrx1* and *TsPrx3*), were cloned. The sequence of the proteins suggests that both isoforms belong to the class of typical Prxs 2-Cys. In addition, *TsPrx3* harbors a mitochondrial localization signal peptide and two motifs (-GGLG- and -YP-) associated with overoxidation. Our kinetic characterization assigns them as thioredoxin peroxidases (TPxs). While *TsPrx1* and *TsPrx3* exhibit the same catalytic efficiency, thioredoxin–glutathione reductase from *T. crassiceps* (*TcTGR*) was five and eight times higher. Additionally, the latter demonstrated a lower affinity (>30-fold) for H₂O₂ in comparison with *TsPrx1* and *TsPrx3*. The *TcTGR* contains a Sec residue in its C-terminal, which confers additional peroxidase activity. The aforementioned aspect implies that *TsPrx1* and *TsPrx3* are catalytically active at low H₂O₂ concentrations, and the *TcTGR* acts at high H₂O₂ concentrations. These results may explain why the *T. crassiceps* cysticerci can tolerate high H₂O₂ concentrations.

Keywords: peroxiredoxins; *Taenia crassiceps*; thioredoxin–glutathione reductase; hydrogen peroxide



Citation: Guevara-Flores, A.; Nava-Balderas, G.; de Jesús Martínez-González, J.; Vásquez-Lima, C.; Rendón, J.L.; del Arenal Mena, I.P. A Physiological Approach to Explore How Thioredoxin–Glutathione Reductase (TGR) and Peroxiredoxin (Prx) Eliminate H₂O₂ in Cysticerci of *Taenia*. *Antioxidants* **2024**, *13*, 444.

<https://doi.org/10.3390/antiox13040444>

Received: 1 February 2024

Revised: 2 April 2024

Accepted: 4 April 2024

Published: 10 April 2024



Copyright: © 2024 by the authors. Licensee MDPI, Basel, Switzerland. This article is an open access article distributed under the terms and conditions of the Creative Commons Attribution (CC BY) license (<https://creativecommons.org/licenses/by/4.0/>).

1. Introduction

Reactive oxygen species (ROS) including the superoxide anion, the hydroxyl radical, the O₂ singlet, and hydrogen peroxide (H₂O₂) are among the compounds resulting from aerobic metabolism. H₂O₂ possesses characteristics that reveal its relevance inside cells, such as the following: (I) it has no charge; (II) it is a very stable molecule compared to other ROS, and consequently, it has the longest half-life; (III) it has the highest diffusion rate, which allows it to diffuse in the whole cell; and (IV) at low concentrations, it acts as a second messenger in signaling pathways [1,2]. To avoid the deleterious accumulation of H₂O₂, organisms rely upon diverse metal-dependent peroxidases, including catalase (CAT) [3] and two thiol-dependent (-SH) antioxidant systems: (a) the glutathione system, composed of glutathione tripeptide (GSH), glutathione reductase (GR), and glutathione peroxidase (GPx), and (b) the thioredoxin system, composed of the small protein thioredoxin (Trx), thioredoxin reductase (TrxR), and peroxiredoxin (Prx). Both thiol-dependent antioxidant systems require NADPH [4]. Together, these systems regulate the H₂O₂ concentration, which maintains an adequate intracellular redox homeostasis in most organisms [5]. It is important to note that CAT is usually confined to peroxisomes [6], and in many endoparasitic organisms like cestodes, this enzyme is absent [7]. In contrast, GPxs and Prxs are

present in most organisms, with different isoforms found in diverse cell compartments [8]. Prxs are characterized mainly by two points: (1) their catalytic efficiency (k_{cat}/K_m) for H_2O_2 is lower ($10^{4-5} \text{ M}^{-1} \text{ s}^{-1}$) [9–11], and this low catalytic efficiency is compensated by (2) their high intracellular concentration that ranges between 15 and 60 μM [12].

All Prxs depend on the presence of a catalytic cysteine around position 50 (Cys^{50}) that reacts with H_2O_2 ; identified as peroxidatic cysteine ($\text{C}_\text{P}\text{SH}$). Based on this, Prxs are most often classified by the number of catalytic cysteine residues per subunit. Prxs with one cysteine (Prx 1-Cys) and two cysteines (Prx 2-Cys) exist. For Prx 2-Cys, the second cysteine (Cys^{170}) was identified as the resolving cysteine ($\text{C}_\text{R}\text{SH}$) [13,14]. The reduction of H_2O_2 is performed through the oxidation of $\text{C}_\text{P}\text{SH}$ to sulfenic acid ($\text{C}_\text{P}\text{SOH}$); subsequently, this sulfenic acid reacts with $\text{C}_\text{R}\text{SH}$, generating a disulfide bond ($\text{C}_\text{P}\text{S}-\text{S}_\text{C}_\text{R}$). When this disulfide bond is intermolecular, the Prxs are “typical”, and when it occurs in the same subunit, they are described as “atypical” [15]. In both cases, the disulfide bond is generated anew to its dithiol form by the reduced forms of thioredoxin ($\text{Trx}-(\text{SH})_2$) or glutathione (GSH) [16]. A shared feature by most Prxs is that they are sensitive to overoxidation, with micromolar concentrations of H_2O_2 , and are known as “sensitive Prxs” [16–18]. In sensitive Prxs, two structural motifs (-GGLG- and -YP-) have been described that are predicted to confer sensitivity to H_2O_2 . These sites are highly conserved among the Prxs of eukaryote cells; however, recently, “robust Prxs” (resistant to overoxidation) have been reported in bacteria including *Escherichia coli* and *Salmonella*, which lack these motifs and instead harbor two highly conserved motifs that have been associated with resistance to H_2O_2 [19]: (A and B: -D(N/G)H(G/S)- and -T(S/T)-, respectively).

The enzymatic activity of Prxs was determined with an assay coupled with TrxR and Trx using as reducer to NADPH. Generally, for this assay, the enzyme coupling of *E. coli* [20,21] and yeast [22] are the most used. These organisms’ reductases lack a Sec residue, so their TrxR is termed TrxR-Cys. Markedly, endogenous proteins were used to determine the activity of Prxs for a few organisms, like *Plasmodium falciparum* (*Pf*TrxR-Cys and *Pf*Trx) [23]. The eukaryotic TrxRs are selenocysteine-dependent (termed TrxR-Sec) and generally have the capacity to recognize Trxs of another origin as substrates [24], whereas the TrxR-Cys of prokaryotes are usually highly specific for their own endogenous Trx [24,25]. On the other hand, the specificity of Prxs for Trxs of other origins is not well documented. This information is relevant to establish which system is more appropriate to determine the activity of Prxs in a physiological context.

Parasite plathelminths of the cestode class must have a robust mechanism for the depuration of ROS that are either generated by the host’s immunological system [26] or from their own metabolism [26,27]. Studies performed in *Taenia crassiceps* have demonstrated significant amounts of H_2O_2 production under basal conditions [28], and the larval form can tolerate exposure to higher concentrations of H_2O_2 in culture conditions [29]. However, it is widely documented in diverse parasitic platyhelminths at both the genomic and proteomic levels that cestodes lack CAT, TrxR, and GR [7,30]; hence, their redox homeostasis relies on a bifunctional enzyme: the thioredoxin–glutathione reductase (TGR-Sec), which is the sole enzyme responsible for maintaining both thioredoxin and glutathione in their reduced state. Regarding the thiol-dependent peroxidases, a gene that encodes a GPx has been previously described in the *Taenia solium* genome, which is predicted to be associated with the plasma membrane [31], as well as two genes that encode 2-Cys Prxs isoforms [31].

This work aimed to identify the factors involved in the high tolerance of the *Taenia* genus to millimolar concentrations of H_2O_2 . In this study, two Prxs of the *T. solium* cysticerci were cloned and expressed. Here, we characterize how they remove H_2O_2 using their endogenous thioredoxin system and the role of *T. crassiceps* cysticerci (*Tc*) TGR-Sec in this process.

2. Materials and Methods

2.1. Chemicals

NADPH, H₂O₂, ter-butyl hydroperoxide solution (Luperox), cumene hydroperoxide, Trizol[®], bacto yeast, bacto tryptone, IPTG, ampicillin, and chloramphenicol, as well as Tris, EDTA, oxidized glutathione (GSSG), reduced glutathione (GSH), PMSF, manganese (II) chloride, L-glutamine, hydroxylamine, ADP, DEAE-cellulose, HA-Ultrogel, and Cibacron Blue 3G-A were obtained from Sigma-Aldrich, Merck KGaA, (Darmstadt, Germany). All other chemicals were purchased from JT Baker Chemical, Phillipsburg, NJ, USA.

2.2. Biological Material

T. solium cysticerci were obtained from the skeletal muscle of naturally infected pigs from City of Cuautla, State of Morelos, México. The cysticerci were washed with phosphate buffer (PBS), pH 7.4, and frozen until use. *T. crassiceps* cysticerci (HYG strain) were obtained from the peritoneum of experimentally infected BALB/c mice as described [32], washed with PBS, and frozen until use. All animal care and research protocols were carried out in accordance with the guidelines for the ethical care of experimental animals according to the guidelines of the Official Mexican Standards for the production, care, and use of laboratory animals (NOM-062-ZOO-1999). Further, the experimental protocols reported in the present work were approved by the Internal Committee for the Care and Use of Laboratory Animals (CICUAL) of the Facultad de Medicina, Universidad Nacional Autónoma de México (008-CIC-2023). All efforts were made to minimize animal suffering and to reduce the number of animals used.

2.3. Cloning and Overexpression of TsPrx1 and TsPrx3

Plasmid pET-23a (+) was obtained from Novagen[®], Merck KGaA group (Darmstadt, Germany). *E. coli* strains TOP10 and BL-21 Codon Plus (DE3) were purchased from the Invitrogen corporation (Carlsbad, CA, USA). The plasmid purification kit was obtained from Thermo-Scientific (Waltham, MA, USA), as were the NdeI and Xho I restriction enzymes and the RevertAid First Strand synthesis kit used to obtain the cDNA. The amplified (TAQ DNA polymerase) was obtained from BioTecMol (Mexico City, Mexico). T4 DNA ligase was purchased from Promega Corporation (Madison, WI, USA), and the GelRed[®] was obtained from Biotium (Fremont, CA, USA). Trx from *E. coli*, Trx from humans, TrxR from rats, TrxR from *E. coli*, and GR from *yeast*, were obtained from Sigma-Aldrich.

Two Prxs coding sequences were identified in the WormBase Parasite (https://parasite.wormbase.org/Taenia_solium_prjna170813/Info/Index/, accessed on 2 August 2022): TsPrx1 (22 kDa) [33] and TsPrx3 (25 kDa). The total RNA from three *T. solium* cysticerci was extracted with TriZol[®], and the cDNA synthesis was carried out using the RevertAid First Strand synthesis kit (Thermo Scientific, Waltham, MA, USA) with the supplier's specifications and using oligo (dT)₁₂ primer (5 µM final concentration). The synthesized cDNA (2 µL) was used as a template to amplify the Prxs genes by means of PCR reactions (50 µL total volume), using 100 ng/µL (0.2 µM) of each oligonucleotide 5'-ATTCATATGGCTGCTGCTGTCATCGGG-3' and 3'-AAACTCGAGTCTTGAGCTCATGACGAC-5' for the TsPrx1 isoform; for TsPrx3, the oligonucleotides 5'AAGCATATGCAGCGTCTTATGCCTCATC-3' and 3'TATCTCGAGGTTGACCTTCTCAAAGTACGC-5' were used. The PCR reactions were carried out at an initial incubation temperature of 94 °C for 30 s; the alignment temperature was 61 °C for 35 s, and the extension temperature was 72 °C for 90 s; the final extension temperature was 72 °C for 10 min. PCR products were analyzed by electrophoresis on a 1.5% agarose gel with known molecular weight (MW) markers and visualized with GelRed[®] at λ = 312 nm; the products were purified and sequenced via the Sanger method [34] at the Sequencing Unit of the Institute for Biomedical Research (IIB, Cuernavaca, Morelos, Mexico). The resultant sequences were aligned and compared with the sequences of TsPrx1 and TsPrx3 identified in the GeneBank database, using the NCBI BLAST page (<https://blast.ncbi.nlm.nih.gov/>), accessed on 29 September 2023.

The amplified *TsPrx1* and *TsPrx3* genes were cloned into the pET-23a(+) expression vector (Novogen, Dublin, Ireland), using the *NdeI* and *XhoI* cutting sites. The constructs were used to transform *E. coli* TOP 10 and Codon Plus bacteria. Positive clones were identified by PCR reactions with the specific oligos. Codon Plus positive bacterial clones were grown in LB culture (Luria–Bertani) with ampicillin (0.1 mg/mL) and chloramphenicol (34 µg/mL). The induction of the expression of clones *TsPrx1* and *TsPrx3*, both with His tags in their amino terminal ends, was carried out by adding 1 mM IPTG at 37 °C and 300 rpm. After 4 h of incubation, bacteria were recovered by centrifugation and lysed by sonication at a frequency of 20 KHz. The expression of *TsPrx* was confirmed by SDS-PAGE according to Laemmli [35] and stained with Coomassie blue. The *Prxs* were purified from the soluble bacterial lysate by affinity chromatography on IMAC Sepharose (BioRad, Hercules, CA, USA). The protein concentration was determined with the extinction coefficient (ϵ) of each protein [36].

2.4. Purification of the TGR from *T. crassiceps* and Recombinant Trx from *T. solium*

The protocol followed in the purification of cytosolic TGR from *T. crassiceps* has been described elsewhere [37], using 20 infected mice (around 400 cysticerci per mouse). The recombinant Trx from *T. solium* was obtained following the protocol previously described [38].

2.5. Bioinformatics Analysis

The amino acid sequence alignment of *TsPrx1* and *TsPrx3* was performed using the Clustal Omega program (<https://www.uniprot.org/align/>, accessed on 19 October 2022). The prediction of the subcellular location of an N-terminal peptide corresponding to *TsPrx3* was performed using DeepLoc-1.0 (<https://services.healthtech.dtu.dk/services/DeepLoc-1.0/>, accessed on 6 June 2023) and resulted in being mitochondrial-directed.

2.6. Electrophoresis

Polyacrylamide gel (4, 10, and 16%) electrophoresis under denaturing conditions was performed as described by Shägger [39]. Gels were stained by conventional procedures. The purity degree of the *TsPrx1*, *TsPrx3*, Trx proteins from *T. solium* and the TGR from *T. crassiceps* was established by analyzing the densitometry of each protein in the SDS-PAGE using ImageJ (<https://imagej.nih.gov/ij/>), accessed on 8 November 2023.

2.7. Protein Determination

The concentration of *TsPrx1*, *TsPrx3*, and *TsTrx* was determined by measuring their absorbance at 278 nm. The corresponding extinction coefficients (ϵ) were as follows: *TsPrx1* = 20.6 mM⁻¹ cm⁻¹; *TsPrx3* = 21.4 mM⁻¹ cm⁻¹; and *TsTrx* = 7.8 mM⁻¹ cm⁻¹. For *TcTGR*, its protein concentration was determined at 460 nm based on its FAD content (ϵ = 11.3 mM⁻¹ cm⁻¹). The protein concentration was corroborated by the densitometric method [40].

2.8. Enzyme Assays

This section pertains to the thioredoxin reductase activity of *TcTGR*. The reductase activity was determined by following the decrease in absorbance at 340 nm due to the oxidation of NADPH (150 µM) in the presence of recombinant *TsTrx*. Assays were performed at 25 °C in 100 mM Tris-HCl buffer (pH 7.8) containing 1 mM EDTA (TE buffer) in a final volume of 0.6 mL. The reaction was started by adding insulin (to recycle *TsTrx*) at a final concentration of 25 µM. An extinction coefficient of 6.22 mM⁻¹ cm⁻¹ for NADPH was used for the calculations of enzyme activity, as described previously [37].

Here, the activity of the peroxiredoxins from *T. solium* is discussed. This activity was determined by either of the two methods described below. The final volume of the reaction mixture was 0.3 mL. Unspecific rates were subtracted from the specific rates. All activity assays were carried out in a UV/Vis spectrophotometer DU-730 from Beckman Coulter.

2.8.1. Peroxidase Activity Assays

The reductase activity of the recombinant Prxs using either H₂O₂ or organic hydroperoxides (cumene hydroperoxide and *t*-butyl hydroperoxide) as oxidizing substrates was determined in TE buffer by following the oxidation of 150 μM NADPH at 340 nm and 25 °C in a coupled assay with TcTGR (11.2 nM), TsPrx1 or TsPrx3 (1.25 μM) and recombinant TsTrx (60 μM), and the latter was tested as a reductant substrate; under these conditions, when the maximum reduction was obtained (baseline), the specific reaction was started by adding the corresponding peroxide. One unit of Prx activity was defined as the amount of enzyme required to cause the oxidation of 1 nmol of NADPH per minute under the assay conditions described. Alternatively, the peroxidase activity with GSH as the reductant was assayed with GR from *Saccharomyces cerevisiae* or TcTGR (own reductase). The reaction mixture contained the following: (a) 0.1 unit/mL ScGR (Sigma) or (b) 11.2 nM TcTGR, 150 μM NADPH, 1.25 μM of TsPrx1 or TsPrx3, and 1 mM GSH in a buffer containing 100 mM sodium phosphates (pH 7.0), 1 mM EDTA. The reaction was initiated by adding the corresponding peroxide, and the consumption of NADPH was recorded by following the decrease in absorbance at 340 nm and 25 °C.

2.8.2. Thioredoxin Peroxidase Activity of TcTGR and EcTrxR

The comparison of a selenocysteine-dependent enzyme (TcTGR) with a Cys-dependent enzyme (EcTrxR), regarding its ability to catalyze the Trx-dependent reduction of H₂O₂, was evaluated by mixing 150 μM NADPH with either 60 μM TsTrx and 11.2 nM TcTGR or 6 μM EcTrx and 83 nM EcTrxR in TE buffer. The reaction was started by adding 1 mM H₂O₂, and the absorbance at 340 nm was measured. The final volume of the reaction mixture was 0.6 mL.

The kinetic constants K_m and k_{cat} of TsPrx1 and TsPrx3 for either H₂O₂, *t*-butyl hydroperoxide, or the cumene hydroperoxide substrates were determined by varying the concentration of the corresponding peroxide at a constant concentration of both NADPH (150 μM) and TsTrx (60 μM). To obtain the kinetic parameters for TsTrx, a constant concentration of 50 μM H₂O₂ was used at varying TsTrx concentrations. In all cases, fixed concentrations of TsPrxs (1.25 μM) and TcTGR (11.2 nM) were used (these last concentrations were previously determined to prevent them being limiting). The kinetic constants of TcTGR toward H₂O₂ was obtained by varying the concentration of the peroxide at a constant concentration of NADPH (150 μM) and TsTrx (60 μM). All initial velocity data were fitted to the Michaelis–Menten equation through non-linear regression analysis using Sigma-Plot Software version 12.

2.8.3. Glutamine Synthetase Protection Assay

The ability of cytosolic TcTGR, TsPrx1, and mitochondrial TsPrx3 to protect glutamine synthetase (GS) from oxidation was performed as previously described [41]. For both TsPrx1 and TsPrx3, the inactivation mixture contained 0.15 μM GS from *E. coli*, 3 μM FeCl₃, and 10 mM DTT either in the presence or in the absence of 1.25 μM of the corresponding Prx in 50 mM HEPES buffer (pH 7). The final volume of the mixture was 50 μL. For TcTGR, the inactivation mixture additionally contained 160 μM NADPH and recombinant TsTrx either in the presence or in the absence of TcTGR. After 15 min of incubation at 30 °C, the residual activity of GS was determined by adding 1 mL of the assay mixture (0.4 mM ADP, 0.15 M glutamine, 10 mM Na₂HAsO₄, 20 mM NH₂OH, and 0.4 mM MnCl₂ in 100 mM HEPES buffer), pH 7.4. The resultant solution was incubated for 30 min at 30 °C; then, the reaction was terminated by adding 0.25 mL of stop mixture (0.3 M FeCl₃ and 5.8 M HCl), and the formation of the γ-glutamylhydroxamine-Fe³⁺ complex was measured at 540 nm.

2.9. Data Presentation and Statistical Analysis

The data shown below represent the mean ± S.D. of three independent experiments. Data were evaluated for statistical significance using Student's *t*-test and Statistical Software OriginPro (version 8, OriginLab Corporation, Northampton, MA, USA).

3.2. Purity Degree of Recombinant Proteins

The degree of purity of *TsPrx1* and *TsPrx3* and *TsTrx* recombinant proteins, and that of *TcTGR*, was determined through electrophoresis in denaturing conditions (SDS-PAGE). Figure 2 shows that the four proteins had a significant degree of purity, which was confirmed through densitometry analysis of each band, revealing a purity greater than 75% for all proteins.

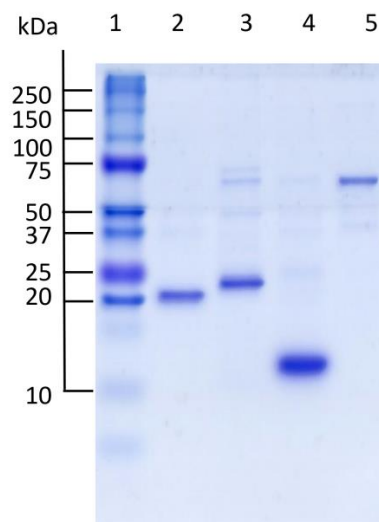


Figure 2. Electrophoretic patterns of thioredoxin system proteins from the *Taenia* genus. Proteins were obtained from the different purification protocols. Lanes are as follows: lane 1, MW markers; lane 2, *TsPrx1* (8.0 µg); lane 3, *TsPrx3* (10.6 µg); lane 4, *TsTrx1* (5.3 µg); lane 5, *TcTGR* (4.4 µg). Purity grade determined by densitometry for *TsPrx1* (87%), *TsPrx3* (81%), *TsTrx* (85%), and *TcTGR* (75%).

3.3. Peroxidase Activity of the Recombinant *TsPrx1* and *TsPrx3*

Based on results (see below), 60 µM of *TsTrx* was used in the activity assays, one and a half times the K_m for *TcTGR*. For GSH, 1 mM of GSH was used, which corresponds to the concentration reported in *T. crassiceps* cysticerci [27]. The activity of *TsPrx1* and *TsPrx3* was determined by changing the concentration of H_2O_2 (Table 1).

Table 1. Kinetic constants of recombinant *TsPrx1* and *TsPrx3* toward H_2O_2 in the presence of Trx.

Enzyme	Hydrogen Peroxide			
	Reducing Substrate	K_m (M)	k_{cat} (s^{-1})	k_{cat}/K_m ($M^{-1} s^{-1}$)
<i>TsPrx1</i>	<i>TsTrx</i>	$1.8 \pm 0.5 \times 10^{-6}$	$160 \pm 7.1 \times 10^{-3}$	8.8×10^4
<i>TsPrx3</i>	<i>TsTrx</i>	$1.3 \pm 0.5 \times 10^{-6}$	$90 \pm 4.2 \times 10^{-3}$	6.9×10^4

Data obtained using 150 µM NADPH, 11.2 nM *TcTGR*, 60 µM *TsTrx*, 1.25 µM *TsPrx1*, or *TsPrx3*, and increasing concentrations of H_2O_2 at 25 °C and pH 7.8; data are the means of three independent measurements.

3.4. Kinetic Analysis of *TcTGR*

Kinetic constants of *TcTGR* were determined using *TsTrx* as a substrate with the following results: $K_m = 41.5 \mu M$ and $k_{cat}/K_m = 1.2 \times 10^6 M^{-1} s^{-1}$ (Table S1); despite having different K_m , the catalytic efficiency values were comparable to those reported previously [43] and those reported for *TsTGR* and the recombinant *TsTrx* [38]. Additionally, the comparison of the *TsTGR* gene (ID: TsM_000506200) of the *T. solium* genome submitted in WormBase Parasite database (GENOME ID: PRJNA170813) and the *TcTGR* gene (ID: JAKROA01000003.1) submitted in the GenBank database (GENOME ID: GCA_023375655.1) showed an identity above 90%, and the genomic sequences of the *TsPrx1* and *TcPrx1* genes showed 94% identity [29]. These data suggest that independently of the origin of the proteins used in the activity assays,

either of *T. solium* or *T. crassiceps*, the kinetic parameters were within the same range, and the high rates of identity of the sequences protein or genomics of the different components of the thioredoxin system (TS) enabled us to use *TcTGR* and the recombinant *TsTrx* with confidence in our assays.

Unexpectedly, in Figure S2, it is shown that when using GSH as substrate, it was not possible to detect the peroxidase activity in *TsPrx1* and *TsPrx3* in the presence of *ScGR* or *TcTGR* in the coupled assay (as mentioned under Materials and Methods Section 2). Tables 1 and S2 show that the two Prxs depict a high affinity for different peroxides ($K_m < 8.4 \mu\text{M}$), except for *TsPrx1*, whose affinity for the *t*-butyl hydroperoxide was significantly lower ($K_m = 18.1 \mu\text{M}$). The catalytic efficiency for the different peroxides was about $\sim 10^4 \text{ M}^{-1} \text{ s}^{-1}$; these kinetic parameters were within the same order of magnitude as other Prxs [10,11].

Peroxidase activity was not detected using GSH and with other organic peroxides as oxidizing substrates. Afterward, the kinetic constants for both Prxs toward the Trx were determined at a constant concentration of $50 \mu\text{M}$ of H_2O_2 . The results obtained are shown in Table 2. It is interesting to point out that the affinity of *TsPrx3* for *TsTrx* was significantly lower compared to that of *TsPrx1*. Again, GSH was not efficient as a reducer.

Table 2. Kinetic constants for recombinant *TsPrx1* and *TsPrx3* for *TsTrx*.

Enzyme	<i>TsTrx</i>		
	K_m (M)	k_{cat} (s^{-1})	k_{cat}/K_m ($\text{M}^{-1} \text{ s}^{-1}$)
<i>TsPrx1</i>	$38.6 \pm 1.8 \times 10^{-6}$	$160 \pm 4.0 \times 10^{-3}$	4.1×10^3
<i>TsPrx3</i>	$122.0 \pm 14.5 \times 10^{-6}$	$100 \pm 7.3 \times 10^{-3}$	0.8×10^3

Measurements obtained as described under Materials and Methods Section 2; data are the means of three independent measurements.

3.5. Dependence of the Peroxidase Activity of *TsPrx1* and *TsPrx3* on the H_2O_2 Concentration

As mentioned, only *TsPrx3* has the two motifs that provide sensitivity to H_2O_2 in its sequence. To determine the susceptibility of both Prxs to H_2O_2 , peroxidase activity was analyzed with a wide range of H_2O_2 concentrations. Figure 3 shows the saturation curves of both enzymes with a clear biphasic pattern, suggesting the presence of two components with peroxidase activity. A comparison of the two activity profiles reveals that the apparent maximal velocity of the component with the highest affinity is higher for the assays with *TsPrx1*.

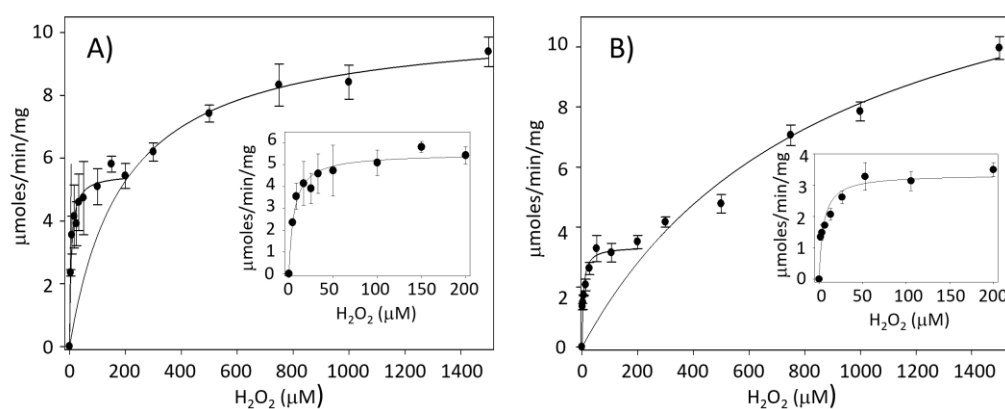


Figure 3. Two enzymes with peroxidative activity. (A) *TsPrx1* and *TcTGR*, Michaelis–Menten plot; (insert) magnification of the lower concentrations $< 200 \mu\text{M}$ H_2O_2 and (B) *TsPrx3* and *TcTGR*. The graphs were adjusted to protein concentration of *TcTGR* [11.2 nM] as well as *TsPrx1* and *TsPrx3* [$1.25 \mu\text{M}$]. Data are the means of three independent measurements.

However, in both cases, the total maximal velocity is essentially identical. A non-linear regression analysis yielded the corresponding kinetic parameters for both systems (Table 3). Because *TcTGR* is present as an auxiliary enzyme in the activity assays of both *TsPrxs*, it is possible that one of the components observed in the saturation graphs could be due to *TcTGR*. Consequently, the potential activity of the peroxidase of *TcTGR* was analyzed in the absence of *TsPrxs* (Figure S3). The results revealed that the peroxidase activity of *TcTGR* is significant (K_m : 79.8 μM), overlapping with the activity observed in the assays performed in the presence of *TsPrx1*. Therefore, it can be concluded that the main contribution of the peroxidase activity is exerted by *TcTGR*, particularly at high H_2O_2 concentrations. Despite its significantly lower affinity for the peroxide, the catalytic efficiency of *TcTGR* is approximately five and eight times higher than that of *TsPrx1* and *TsPrx3*, respectively (Table 3).

Table 3. Kinetic constants for H_2O_2 reduction by recombinant *TsPrx1* and *TsPrx3* and by *TcTGR*.

Hydrogen Peroxide				
Enzyme	Thioredoxin System	K_m (M)	k_{cat} (s^{-1})	k_{cat}/K_m ($\text{M}^{-1} \text{s}^{-1}$)
<i>TsPrx1</i> *	<i>TcTGR</i> + <i>TsTrx</i>	$5.8 \pm 1.0 \times 10^{-6}$	$64 \pm 2.1 \times 10^{-3}$	1.0×10^4
<i>TsPrx3</i> **	<i>TcTGR</i> + <i>TsTrx</i>	$4.9 \pm 1.2 \times 10^{-6}$	$35 \pm 1.9 \times 10^{-3}$	0.7×10^4
<i>TcTGR</i> *	<i>TsPrx1</i> + <i>TsTrx</i>	$192.0 \pm 16.1 \times 10^{-6}$	$11,200 \pm 230.0 \times 10^{-3}$	5.8×10^4

Data obtained using 150 μM NADPH, 60 μM *TsTrx*, 11.2 nM *TcTGR*, 1.25 μM *TsPrx1*, and increasing concentrations of H_2O_2 (2–1500 μM) at 25 °C and pH 7.8; * data obtained from the Michaelis–Menten graph of two enzymes with peroxidase activity (Figure 3A and insert). Lines one and three (cytosolic *TsPrx1* and *TcTGR*); ** data obtained from the Michaelis–Menten graph of two enzymes with peroxidase activity (Insert, Figure 3B). Line two (mitochondrial *TsPrx3*).

3.6. Peroxidase Activity of *TrxR* of *E. coli*

To determine whether the selenocysteine (Sec) residue plays a critical role in the high peroxidase activity of the TGR, its activity was compared to that of a *TrxR* lacking such residue, using the enzyme of *E. coli*. The results (Figure 4) revealed that the peroxidase activity of *TcTGR* was significantly higher ($9.4 \mu\text{mol min}^{-1} \text{mg}^{-1}$) compared with that of *EcTrxR* ($0.47 \mu\text{mol min}^{-1} \text{mg}^{-1}$).

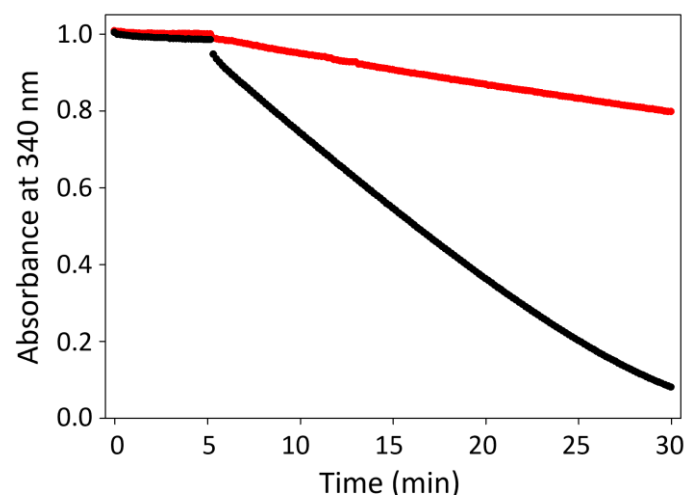


Figure 4. Influence of Sec or Cys residues in hydroperoxide reductase activity. The ability to reduce hydroperoxide of *TcTGR*-Sec (in black) and *EcTrxR*-Cys (in red) was determined. Measurements obtained as described under Materials and Methods Section 2. Black line: 11.2 nM *TcTGR* and 60 μM *TsTrx*, and red line: 83 nM *EcTrxR* and 6 μM *EcTrx*, and 1 mM H_2O_2 was added to start the reaction. The decrease in absorbance at 340 nm was recorded.

3.7. Protection of the Glutamine Synthetase

The peroxidase activity present in the *Tc*TGR or *Ts*Prxs and their consequent protective activity of the GS from ROS was compared. As shown in Figure 5A, in the presence of TS (NADPH + *Ts*Trx + *Tc*TGR), ~50% protection was obtained. The addition of *Ts*Prx1 resulted in ~80% protection, whereas *Ts*Prx3 did not protect and had the same magnitude regarding protection as TS (Figure 5B).

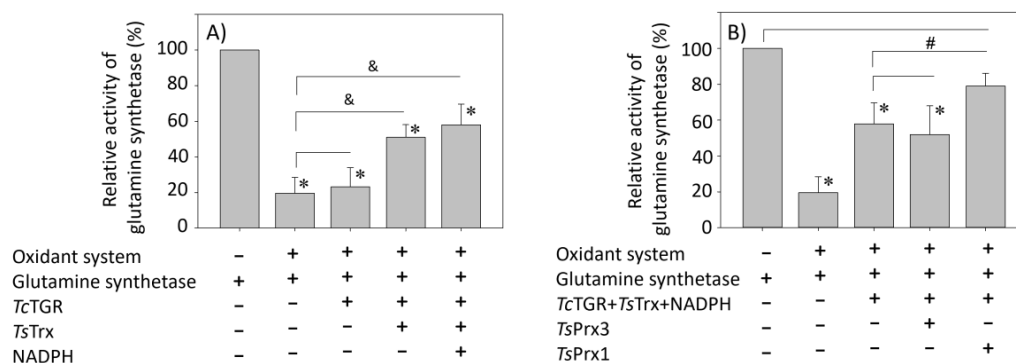


Figure 5. Protection of glutamine synthetase by the different components of thioredoxin system and by the *Ts*Prx1, *Ts*Prx3, and *Tc*TGR enzymes. The different components of TS: *Tc*TGR (11.2 nM), *Ts*Trx (60 μ M), NADPH (100 μ M), *Ts*Prx1 (1.25 μ M), or *Ts*Prx3 (1.25 μ M) were incubated with GS from *E. coli* (150 nM) in the presence of a mixed-function oxidation system (OS) in a final volume of 50 μ L. After 15 min, 2 mL of the γ -glutamyl transferase assay mixture were added. Additional details are described under Materials and Methods Section 2. (A) TS bar 1, positive control; bar 2, negative control; bar 3, mixture without *Ts*Trx and NADPH; bar 4, mixture without NADPH; bar 5, full mixture. (B) Enzymes *Ts*Prx1, *Ts*Prx3, and *Tc*TGR. Bar 1, positive control; bar 2, negative control; bar 3, full mixture with *Tc*TGR; bar 4, full mixture with *Ts*Prx3; and bar 5, full mixture with *Ts*Prx1. Statistical significance was considered at a p -value < 0.05, as indicated: * = comparison between the different components of the TS vs. GS activity control; & = comparison between the different components of the TS vs. GS residual activity in the presence of the OS; # = comparison between TS vs. *Ts*Prx1 or *Ts*Prx3.

4. Discussion

Peroxioredoxins, enzymes that reduce H_2O_2 , are widely represented among organisms [44]. A search in the *T. solium* genome revealed that this parasite possesses two peroxiredoxins: *Ts*Prx1 and *Ts*Prx3. The sequence analysis of both Prxs was performed, and the *Ts*Prx3 sequence showed the presence of a signaling peptide, suggesting its localization to mitochondria (Figure S1). Both sequences indicated that they could be classified within the “typical Prx 2-Cys” group (Figure 1). The *Ts*Prx3 isoform harbored the motifs (-GGLG-) and (-YP-) associated with the hyperoxidation produced by H_2O_2 [16,17]. Interestingly, the presence of these motifs in *Ts*Prx3 did not confer a higher or lower kinetic behavior compared to *Ts*Prx1. Both peroxiredoxins could recognize H_2O_2 with a catalytic efficiency of $\sim 10^4 M^{-1} s^{-1}$ (Table 1), which is comparable to other organic peroxides (Table S2) used in the present work as substrates.

*Ts*Prx’s affinity for H_2O_2 is clearly higher if compared with the Prxs of the *Schistosoma mansoni* trematode [20]. However, its catalytic efficiency is comparable to those reported for the Prxs of diverse organisms, such as the *H. contortus* nematode [42], *Bacillus subtilis* [45], and *Helicobacter pylori* [46], which reduce H_2O_2 using only Trx-(SH)₂ and do not recognize GSH. In contrast, Prxs that can use both GSH and Trx-(SH)₂ have been reported in *P. falciparum* [23,47], *S. mansoni* [20], and *Clonorchis sinensis* [21]. It is interesting to point out that among Prxs that use both reducing substrates, some, including *P. falciparum* and *S. mansoni*, use GSH more efficiently as a substrate. The results of this work indicate that GSH cannot serve as a reducing substrate and therefore is a marked preference for Trx-

(SH)₂; hence, we suggest that both *TsPrx1* and *TsPrx3* must be considered true thioredoxin peroxidases (TPx).

In Prx 2-Cys the C_PSH thiol can reach different states of oxidation by reacting sequentially with one, two, or three H₂O₂ molecules, giving rise sequentially to sulfenic (C_PSOH), sulfinic (C_PSO₂H), and sulfonic (C_PSO₃H) acids. The reaction needed to generate the C_PSO₂H is reversible through an ATP-dependent sulfiredoxin (Srx), whereas the reaction that generates the C_PSO₃H is irreversible [11,17]. The overoxidation of this thiol promotes the Prx to restructure and generate decamer-type oligomers (five homodimers, also known as “toroids”). At this point, the antioxidant activity of the Prx diminishes, favoring its transformation into a protein with a chaperone function. Only “typical” Prxs are believed to generate this type of oligomer [44] due to the presence of the motifs sensitive to H₂O₂, which are absent in *TsPrx1* (Figure 1). This suggests that *TsPrx1* could be a robust Prx similarly to that of the Prx (AhpC) of *Salmonella typhimurium* [19].

As previously mentioned, the low peroxidase activity of the Prxs could be related to the fact that the catalytic residues are cysteines [16,17,44], in contrast with those GPx selenium-dependent (GPx-Sec), which are generally more active [47]. The insertion of a Sec residue in a protein through site-directed mutagenesis enables enzymes to use a greater spectrum of substrates, including H₂O₂. In addition, the substitution of the essential serine residue by a Sec residue (Ser/Sec) in the subtilisin protease led to a loss of its original activity and the acquisition of a peroxidase activity [48]. A similar result was obtained for the GPx-Sec: the substitution of Sec residue with a Cys residue drastically reduced its activity and increased its sensitivity to overoxidation by H₂O₂ [49]. In our study, we found that *TcTGR* possesses an essential Sec residue that is likely responsible for its high peroxidase activity (Figure 4). Calculations of the initial velocity, using H₂O₂ as a substrate, revealed a 20 times higher activity compared to the activity of *EcTrxR*. These data support the important role of the Sec residue in the peroxidase activity of this enzyme.

The results shown in Figure 3 and Table 3 reveal that *TcTGR* contributes greatly to reduce H₂O₂. This suggests that when the assay system contains TGR and Prx, the peroxidase activity observed at low H₂O₂ concentrations is due mainly to *TsPrx1* and *TsPrx3*, whereas at high concentration of the peroxide, where *TsPrxs* are already saturated, the reducing activity must be attributed to *TcTGR*. Additionally, in the intact organism, the TGR and its corresponding Prx coexist physiologically and are present in both cytosol and mitochondria; hence, their relative participation in peroxides depuration will depend not only on their kinetic parameters but also on the concentration in each organelle. In this sense, it is well known that the peroxiredoxins represent an important fraction of the total protein in a large variety of organisms, reaching up to 1% of the total soluble protein [44]. In this case, in the cestodes, it will be necessary to assess the concentration of these enzymes in intact organisms to obtain conclusive evidence about their relative importance in H₂O₂ depuration. We found no significant differences in the kinetic parameters for *TsPrxs1* and *TsPrx3*, under the conditions used in this study. However, we found differences between the two Prxs in the GS protection assay (Figure 5). *TsPrx3* does not protect GS from oxidative damage, possibly because this isoform harbors the motifs sensitive to overoxidation. On the other hand, *TcTGR* and *TsPrx1* do protect GS from oxidative damage.

As mentioned in the Introduction, *T. crassiceps* cysticerci can tolerate high H₂O₂ concentrations in the millimolar range [28,29]. Although, under physiological conditions it is barely probable to reach such levels, the kinetic characteristics described for *TcTGR* ($K_m \sim 200 \mu\text{M}$ by H₂O₂ and $V_{max} \sim 10.36 \mu\text{mol min}^{-1} \text{mg}^{-1}$) seem to have evolved to work in the presence of moderately high H₂O₂ concentrations. *TsPrxs1* and *TsPrx3* have significantly higher affinities for the peroxide, compared with *TcTGR* (Table 3), which suggests that these enzymes constitute the first in vivo line of defense to avoid oxidative damage. Although using the *TcTGR* of the parasite in the present work as a coupling enzyme exceeded the activity of *TsPrxs*, its presence in the enzymatic assays reflects a situation closer to the physiological conditions of the parasite where the three enzymes act in the presence of the others. Hence, in these types of parasites, two very efficient systems

have evolved for removing H₂O₂, one cytosolic represented by the cytosolic TGR and Prx1 and another mitochondrial that involves the mitochondrial TGR variant and Prx3.

5. Conclusions

The high peroxidase activity of TGR within TS could explain two relevant aspects in the physiology of the *T. crassiceps* cysticerci: (a) the tolerance of the parasite to millimolar H₂O₂ concentrations [29] and (b) the lack of the CAT gene in trematodes and cestodes [7]. The Prx/Trx/TGR system would compensate for the catalase activity, highlighting TGR's role in redox homeostasis in these two groups of parasites.

Supplementary Materials: The following supporting information can be downloaded at: <https://www.mdpi.com/article/10.3390/antiox13040444/s1>, Figure S1: Prediction of TsPrx3 subcellular localization. Peptide (–MQRLMPHLRPKLFASLSASSHIAPTFQSR–) of TsPrx3 was analyzed using DeepLoc-1.0. (A) Table of predicted subcellular localization. (B) Hierarchical tree; Figure S2: Activity of TsPrx1 and TsPrx3 was determined with the glutathione system. Assays containing 1 mM GSH, 150 μM NADPH, 1.25 μM TsPrx1 (circles) or TsPrx3 (filled circles) were incubated with: (A) 8 nM ScGR (squares) or (B) 11.2 nM TcTGR (squares) in 100 mM Tris/HCl (pH 7.8) 1 mM EDTA for 5 min to allow the reaction to stabilize. H₂O₂ (50 μM) was added to initiate the reaction that was monitored for 6 min at 25 °C; Figure S3: Thioredoxin peroxidase activity of TcTGR. H₂O₂ reduction was measured in the absence of TsPrx1. Measurements obtained as described under Materials and Methods Section 2. Data are the means of three independent measurements; Table S1: Kinetic constants for TsTGR and TcTGR toward recombinant Trx from *T. solium* and Trx from *T. crassiceps*; Table S2: Kinetic constants for recombinant TsPrx1 and TsPrx3 toward hydroperoxides in the presence of TsTrx.

Author Contributions: Conceptualization, A.G.-F. and G.N.-B.; methodology, A.G.-F., G.N.-B. and C.V.-L.; software, A.G.-F.; validation, J.d.J.M.-G., C.V.-L. and J.L.R.; formal analysis, A.G.-F., J.d.J.M.-G., J.L.R. and I.P.d.A.M.; investigation, A.G.-F. and G.N.-B.; resources, I.P.d.A.M.; data curation, I.P.d.A.M., J.d.J.M.-G. and J.L.R.; writing—original draft preparation, A.G.-F. and G.N.-B.; writing—review and editing, A.G.-F., G.N.-B., J.d.J.M.-G., J.L.R., J.d.J.M.-G. and J.L.R.; visualization, A.G.-F. and J.d.J.M.-G.; supervision, I.P.d.A.M.; project administration, I.P.d.A.M.; funding acquisition, I.P.d.A.M. All authors have read and agreed to the published version of the manuscript.

Funding: This work was supported by the research grant IN215223 from Dirección General de Asuntos del Personal Académico (DGAPA) at Universidad Nacional Autónoma de México (UNAM).

Institutional Review Board Statement: All animal care and research protocols were carried out in accordance with the guidelines for the ethical care of experimental animals according to the guidelines of the Mexican Official Standard for the production, care, and use of laboratory animals (NOM-062-ZOO-1999). Further, the experimental protocols reported in the present work were approved by the Internal Committee for the Care and Use of Laboratory Animals (CICUAL) of the Facultad de Medicina, Universidad Nacional Autónoma de México (008-CIC-2023). All efforts were made to minimize animal suffering and to reduce the number of animals used.

Informed Consent Statement: Not applicable.

Data Availability Statement: The authors declare that all data supporting the findings of this study are available within the article and its Supplementary Materials.

Acknowledgments: The authors are grateful to Rachel Duffié (Zuckerman Mind Brain and Behavior Institute, Columbia University, New York, NY, USA) for proofreading the English of the manuscript and to Sandra D. Rodríguez Montañó for technical support.

Conflicts of Interest: The authors declare no conflicts of interest.

References

1. Winterbourn, C.C. Hydrogen peroxide reactivity and specificity in thiol-based cell signalling. *Biochem. Soc. Trans.* **2020**, *48*, 745–754. [CrossRef] [PubMed]
2. Cardoso, A.R.; Chausse, B.; da Cunha, F.; Luévano-Martínez, L.A.; Marazzi, T.B.M.; Pessoa, P.S.; Queliconi, B.B.; Kowaltowski, A.J. Mitochondrial compartmentalization of redox processes. *Free Radic. Biol. Med.* **2012**, *52*, 2201–2208. [CrossRef] [PubMed]
3. Sepasi Tehrani, H.; Moosavi-Movahedi, A.A. Catalase and its mysteries. *Prog. Biophys. Mol. Biol.* **2018**, *140*, 5–12. [CrossRef] [PubMed]

4. Das, K.C.; White, C.W. Redox systems of the cell: Possible links and implications. *Proc. Natl. Acad. Sci. USA* **2002**, *99*, 9617–9618. [[CrossRef](#)]
5. Lennicke, C.; Cochemé, H.M. Redox metabolism: ROS as specific molecular regulators of cell signaling and function. *Mol. Cell.* **2021**, *81*, 3691–3707. [[CrossRef](#)] [[PubMed](#)]
6. Sies, H. Role of Metabolic H₂O₂ Generation. Redox Signaling and Oxidative Stress. *J. Biol. Chem.* **2014**, *289*, 8735–8741. [[CrossRef](#)]
7. Williams, D.L.; Bonilla, M.; Gladyshev, V.N.; Salinas, G. Thioredoxin Glutathione Reductase-Dependent Redox Networks in Platyhelminth Parasites. *Antioxid. Redox Signal.* **2013**, *19*, 735–745. [[CrossRef](#)] [[PubMed](#)]
8. Rhee, S.G.; Woo, H.A.; Kil, I.S.; Bae, S.H. Peroxiredoxin functions as a peroxidase and a regulator and sensor of local peroxides. *J. Biol. Chem.* **2012**, *287*, 4403–4410. [[CrossRef](#)] [[PubMed](#)]
9. Flohé, L.; Budde, H.; Hofmann, B. Peroxiredoxins in antioxidant defense and redox regulation. *BioFactors* **2003**, *19*, 3–10. [[CrossRef](#)] [[PubMed](#)]
10. Gretes, M.C.; Poole, L.B.; Karplus, P.A. Peroxiredoxins in parasites. *Antioxid. Redox Signal.* **2012**, *17*, 608–633. [[CrossRef](#)] [[PubMed](#)]
11. Guevara-Flores, A.; Martínez-González, J.J.; Rendón, J.L.; Del Arenal, I.P. The Architecture of The Antioxidants Systems among Invertebrate Parasites. *Molecules* **2017**, *22*, 259. [[CrossRef](#)] [[PubMed](#)]
12. Andreyev, A.Y.; Kushnareva, Y.E.; Murphy, A.N.; Starkov, A.A. Mitochondrial ROS Metabolism: 10 Years Later. *Biochemistry* **2015**, *80*, 517–531. [[CrossRef](#)] [[PubMed](#)]
13. Barranco-Medina, S.; Lázaro, J.J.; Dietz, K.J. The oligomeric conformation of peroxiredoxins links redox state to function. *FEBS Lett.* **2009**, *583*, 1809–1816. [[CrossRef](#)] [[PubMed](#)]
14. Rhee, S.G. Overview on peroxiredoxin. *Mol. Cells.* **2016**, *39*, 1–5. [[CrossRef](#)] [[PubMed](#)]
15. Nelson, K.J.; Knutson, S.T.; Soito, L.; Klomsiri, C.; Poole, L.B.; Fetrow, J.S. Analysis of the peroxiredoxin family: Using active site structure and sequence information for global classification and residue analysis. *Proteins* **2010**, *79*, 947–964. [[CrossRef](#)] [[PubMed](#)]
16. Wood, Z.A.; Schröder, E.; Robin, H.J.; Poole, L.B. Structure, mechanism, and regulation of peroxiredoxins. *Trends Biochem. Sci.* **2003**, *28*, 32–40. [[CrossRef](#)] [[PubMed](#)]
17. Wood, Z.A.; Poole, L.B.; Karplus, P.A. Peroxiredoxin Evolution and the Regulation of Hydrogen Peroxide Signaling. *Science* **2003**, *300*, 650–653. [[CrossRef](#)] [[PubMed](#)]
18. Hall, A.; Karplus, P.A.; Poole, L.B. Typical 2-Cys peroxiredoxins: Structures, mechanisms, and functions. *FEBS J.* **2009**, *276*, 2469–2477. [[CrossRef](#)] [[PubMed](#)]
19. Bolduc, J.A.; Nelson, K.J.; Haynes, A.C.; Lee, J.; Reisz, J.A.; Graff, A.H.; Clodfelter, J.E.; Parsonage, D.; Poole, L.B.; Furdui, C.M.; et al. Novel hyperoxidation resistance motifs in 2-Cys peroxiredoxins. *J. Biol. Chem.* **2019**, *293*, 11901–11912. [[CrossRef](#)]
20. Sayed, A.A.; Williams, D.L. Biochemical characterization of 2-Cys peroxiredoxins from *Schistosoma mansoni*. *J. Biol. Chem.* **2004**, *279*, 26159–26166. [[CrossRef](#)]
21. Bae, Y.A.; Kim, S.H.; Lee, E.G.; Sohn, W.M.; Kong, Y. Identification, and biochemical characterization of two novel peroxiredoxins in a liver fluke, *Clonorchis sinensis*. *Parasitology* **2011**, *138*, 1143–1153. [[CrossRef](#)] [[PubMed](#)]
22. Kim, J.A.; Park, S.J.; Kim, K.; Rhee, S.G.; Kang, S.W. Activity assay of mammalian 2-Cys peroxiredoxins using yeast thioredoxin reductase system. *Anal. Biochem.* **2005**, *338*, 216–223. [[CrossRef](#)] [[PubMed](#)]
23. Krnajski, Z.; Walter, R.D.; Müller, S. Isolation, and functional analysis of two thioredoxin peroxidases (peroxiredoxins) from *Plasmodium falciparum*. *Mol. Biochem. Parasitol.* **2001**, *113*, 303–308. [[CrossRef](#)]
24. Kanzok, S.M.; Schirmer, R.H.; Turbachova, I.; Lozef, R.; Becker, K. The thioredoxin system of the malaria parasite *Plasmodium falciparum*. Glutathione reduction revisited. *J. Biol. Chem.* **2000**, *275*, 40180–40186. [[CrossRef](#)] [[PubMed](#)]
25. Kanzok, S.M.; Fechner, A.; Bauer, H.; Ulschmid, J.K.; Müller, H.M.; Botella-Munoz, J.; Schneuwly, S.; Schirmer, R.H.; Becker, K. Substitution of the Thioredoxin System for Glutathione Reductase in *Drosophila melanogaster*. *Science* **2001**, *291*, 643–646. [[CrossRef](#)] [[PubMed](#)]
26. Vaca-Paniagua, F.; Torres-Rivera, A.; Parra-Unda, R.; Landa, A. *Taenia solium*: Antioxidant metabolism enzymes as targets for cestocidal drugs and vaccines. *Curr. Top. Med. Chem.* **2008**, *8*, 393–399. [[CrossRef](#)] [[PubMed](#)]
27. Martínez-González, J.J.; Guevara-Flores, A.; Rendón, J.L.; Del Arenal, I.P. Auranofin-induced oxidative stress causes redistribution of the glutathione pool in *Taenia crassiceps* cysticerci. *Mol. Biochem. Parasitol.* **2015**, *201*, 16–25. [[CrossRef](#)] [[PubMed](#)]
28. del Arenal, I.P.; Rubio, M.E.; Ramírez, J.; Rendón, J.L.; Escamilla, J.E. Cyanide-resistant respiration in *Taenia crassiceps* metacystode (cysticerci) is explained by the H₂O₂-producing side-reaction of respiratory complex I with O₂. *Parasitol. Int.* **2005**, *54*, 185–193. [[CrossRef](#)] [[PubMed](#)]
29. Vaca-Paniagua, F.; Parra-Unda, R.; Landa, A. Characterization of one typical 2-Cys Peroxiredoxin gene of *Taenia solium* and *Taenia crassiceps*. *Parasitol. Res.* **2009**, *105*, 781–787. [[CrossRef](#)] [[PubMed](#)]
30. Gupta, A.; Kesharwani, M.; Velmurugan, D.; Tripathi, T. *Fasciola gigantica* thioredoxin glutathione reductase: Biochemical properties and structural modeling. *Int. J. Biol. Macromol.* **2016**, *89*, 152–173. [[CrossRef](#)] [[PubMed](#)]
31. Tsai, I.J.; Zarowiecki, M.; Holroyd, N.; Garciarubio, A.; Sánchez-Flores, A.; Brooks, K.L.; Tracey, A.; Bobes, R.J.; Fragoso, G.; Scitutto, E.; et al. *Taenia solium* Genome Consortium. The genomes of four tapeworm species reveal adaptations to parasitism. *Nature* **2013**, *496*, 57–63. [[CrossRef](#)] [[PubMed](#)]
32. Esquivel-Velázquez, M.; Hernández, R.; Larralde, C.; Ostoa-Saloma, P. Crosstalk among *Taenia crassiceps* (ORF Strain) cysts regulates their rates of budding by ways of soluble and contact signals exchanged between them. *Biomed. Res. Int.* **2014**, *2014*, 703693. [[CrossRef](#)]

33. Molina-López, J.; Jiménez, L.; Ochoa-Sánchez, A.; Landa, A. Molecular cloning and characterization of a 2-Cys peroxiredoxin from *Taenia solium*. *J. Parasitol.* **2006**, *92*, 796–802. [[CrossRef](#)] [[PubMed](#)]
34. Sanger, F.; Coulson, A.R. A rapid method for determining sequences in DNA by primed synthesis with DNA polymerase. *J. Mol. Biol.* **1975**, *94*, 441–448. [[CrossRef](#)] [[PubMed](#)]
35. Laemmli, U.K. Cleavage of structural proteins during the assembly of the head of bacteriophage T4. *Nature* **1970**, *227*, 680–685. [[CrossRef](#)] [[PubMed](#)]
36. Gill, S.C.; von Hippel, P.H. Calculation of Protein Extinction Coefficients from Amino Acids Sequence Data. *Anal. Biochem.* **1989**, *182*, 319–326. [[CrossRef](#)]
37. Rendón, J.L.; del Arenal, I.P.; Guevara-Flores, A.; Uribe, A.; Plancarte, A.; Mendoza-Hernández, G. Purification, characterization, and kinetic properties of the multifunctional thioredoxin-glutathione reductase from *Taenia crassiceps* metacestode (cysticerci). *Mol. Biochem. Parasitol.* **2004**, *133*, 61–69. [[CrossRef](#)]
38. Nava, G.; Maldonado, G.; Plancarte, A. Cloning, expression, purification, and kinetic characterization of mitochondrial thioredoxin (TsTrx2), cytosolic thioredoxin (TsTrx1), and glutaredoxin (TsGrx1) from *Taenia solium*. *Parasitol. Res.* **2019**, *118*, 1785–1797. [[CrossRef](#)] [[PubMed](#)]
39. Shägger, H.; von Jagow, G. Tricine-sodium Dodecyl-sulphate- Polyacrylamide gel electrophoresis for the separation of proteins in the range from 1 to 100 kDa. *Anal. Biochem.* **1987**, *166*, 368–379. [[CrossRef](#)] [[PubMed](#)]
40. Villela, S.M.A.; Kraiem, H.; Bouhaouala-Zahar, B.; Bideaux, C.; Aceves Lara, C.A.; Fillaudeau, L. A protocol for recombinant protein quantification by densitometry. *MicrobiologyOpen* **2020**, *9*, e1027. [[CrossRef](#)]
41. Kim, K.; Kim, H.; Lee, K.Y.; Rhee, S.G.; Stadtman, E.R. The isolation and purification of a specific “protector” protein which inhibits enzyme inactivation by a thiol/Fe(III)/O₂ mixed-function oxidation system. *J. Biol. Chem.* **1988**, *263*, 4704–4711. [[CrossRef](#)] [[PubMed](#)]
42. Hudson, A.L.; Sotirchos, I.M.; Davey, M.W. The activity and hydrogen peroxide sensitivity of the peroxiredoxins from the parasitic nematode *Haemonchus contortus*. *Mol. Biochem. Parasitol.* **2011**, *176*, 17–24. [[CrossRef](#)] [[PubMed](#)]
43. Martínez-González, J.J.; Guevara-Flores, A.; Rendón, J.L.; Sosa-Peinado, A.; Del Arenal Mena, I.P. Purification and characterization of *Taenia crassiceps* cysticerci thioredoxin: Insight into thioredoxin-glutathione-reductase (TGR) substrate recognition. *Parasitol. Int.* **2015**, *64*, 194–201. [[CrossRef](#)] [[PubMed](#)]
44. Sharapov, M.G.; Ravin, V.K.; Novoselov, V.I. Peroxiredoxins as Multifunctional Enzymes. *Mol. Biol.* **2014**, *48*, 600–628. [[CrossRef](#)]
45. Cha, M.K.; Bae, Y.J.; Kim, K.J.; Park, B.J.; Kim, I.H. Characterization of two alkyl hydroperoxide reductase C homologs alkyl hydroperoxide reductase C_H1 and alkyl hydroperoxide reductase C_H2 in *Bacillus subtilis*. *World J. Biol. Chem.* **2015**, *6*, 249–264. [[CrossRef](#)] [[PubMed](#)]
46. Baker, L.M.S.; Raudonikiene, A.; Hoffman, P.S.; Poole, L.B. Essential Thioredoxin-Dependent Peroxiredoxin System from *Helicobacter pylori*: Genetic and Kinetic Characterization. *J. Bacteriol.* **2001**, *183*, 1961–1973. [[CrossRef](#)] [[PubMed](#)]
47. Sztajer, H.; Gamain, B.; Aumann, K.-D.; Slomianny, C.; Becker, K.; Brigelius-Flohé, R.; Flohé, L. The putative glutathione peroxidase gene of *Plasmodium falciparum* codes for a thioredoxin peroxidase. *J. Biol. Chem.* **2001**, *276*, 7397–7403. [[CrossRef](#)] [[PubMed](#)]
48. Mousa, R.; Notis Dardashti, R.; Metanis, N. Selenium and Selenocysteine in Protein Chemistry. *Angew. Chem. Int. Ed. Engl.* **2017**, *56*, 15818–15827. [[CrossRef](#)] [[PubMed](#)]
49. Maroney, M.J.; Hondal, R.J. Selenium versus sulfur: Reversibility of chemical reactions and resistance to permanent oxidation in proteins and nucleic acids. *Free Radic. Biol. Med.* **2018**, *127*, 228–237. [[CrossRef](#)] [[PubMed](#)]

Disclaimer/Publisher’s Note: The statements, opinions and data contained in all publications are solely those of the individual author(s) and contributor(s) and not of MDPI and/or the editor(s). MDPI and/or the editor(s) disclaim responsibility for any injury to people or property resulting from any ideas, methods, instructions or products referred to in the content.